MOLECULAR AND CELLULAR BIOLOGY, Feb. 2007, p. 1455–1466 Vol. 27, No. 4
0270-7306/07/$08.00+0 doi:10.1128/MCB.01369-06

The 14-3-3τ Phosphoserine-Binding Protein Is Required for Cardiomyocyte Survival▽

Jeffrey M. C. Lau, Xiaohua Jin, Jie Ren, Joan Avery, Brian J. DeBosch, Ilya Treskov, Traian S. Lupu, Attila Kovacs, Carla Weinheimer, and Anthony J. Muslin*

Center for Cardiovascular Research, Department of Medicine, Department of Cell Biology and Physiology, Washington University School of Medicine, St. Louis, Missouri 63110

Received 26 July 2006/Returned for modification 15 September 2006/Accepted 24 November 2006

14-3-3 family members are intracellular dimeric phosphoserine-binding proteins that regulate signal transduction, cell cycle, apoptotic, and metabolic cascades. Previous work with global 14-3-3 protein inhibitors suggested that these proteins play a critical role in antagonizing apoptotic cell death in response to provocative stimuli. To determine the specific role of one family member in apoptosis, mice were generated with targeted disruption of the 14-3-3τ gene. 14-3-3$\tau^{-/-}$ mice did not survive embryonic development, but haploinsufficient mice appeared normal at birth and were fertile. Cultured adult cardiomyocytes derived from 14-3-3$\tau^{+/-}$ mice were sensitized to apoptosis in response to hydrogen peroxide or UV irradiation. 14-3-3$\tau^{+/-}$ mice were intolerant of experimental myocardial infarction and developed pathological ventricular remodeling with increased cardiomyocyte apoptosis. ASK1, *c-jun* NH_2-terminal kinase, and p38 mitogen-activated protein kinase (MAPK) activation was increased, but extracellular signal-regulated kinase MAPK activation was reduced, in 14-3-3$\tau^{+/-}$ cardiac tissue. Inhibition of p38 MAPK increased survival in 14-3-3$\tau^{+/-}$ mice subjected to myocardial infarction. These results demonstrate that 14-3-3τ plays a critical antiapoptotic function in cardiomyocytes and that therapeutic agents that increase 14-3-3τ activity may be beneficial to patients with myocardial infarction.

The 14-3-3 family of intracellular phosphoserine-binding proteins regulates many aspects of cell physiology. Initially identified as abundant brain proteins in 1967, 14-3-3 proteins are now recognized as critical regulators of signal transduction cascades, cell cycle checkpoint pathways, apoptotic cascades, and cell metabolism (5, 13). There are seven mammalian isoforms: β, γ, ε, η, σ, τ/θ, and ζ, and they all have broad expression patterns. All 14-3-3 family members bind to phosphoserine-containing motifs, including the RSXSXP motif and RXY/FXSXP motifs, where X is any amino acid (14, 23). 14-3-3 proteins are obligate dimers in cells, and both homo- and heterodimers are formed. The 14-3-3 dimer is able to simultaneously bind to two phosphoserine-containing motifs and therefore may have both scaffolding and adapter functions.

Although many binding partners of 14-3-3 proteins have been identified, a primary function of 14-3-3 proteins may be to block apoptotic pathways. In previous work, we demonstrated that global inhibition of 14-3-3 function, by use of dominant-negative forms of 14-3-3η and 14-3-3ζ that can inhibit the activity of all family members, dramatically lowered the apoptotic threshold of cultured cells or the murine heart (11, 22). Indeed, cardiac-specific expression of dominant-negative 14-3-3η in transgenic mice markedly sensitized those animals to cardiac apoptosis in response to pressure overload by aortic banding (22). In addition, knockdown of 14-3-3τ or 14-3-3ε in *Xenopus laevis* embryos sensitized embryonic cells to apoptotic stimuli (7, 12).

The mechanisms by which 14-3-3 proteins antagonize apoptosis are not completely known, but they include the inhibition of apoptosis signal-regulating kinase 1 (ASK1), a serine/threonine kinase that is activated by tumor necrosis factor alpha, cytokines, hydrogen peroxide, chemotherapeutic agents, and endoplasmic reticulum stress (6, 25). Interestingly, hydrogen peroxide treatment of cultured cells was recently found to result in dephosphorylation of serine-967 of ASK1, which led to dissociation of 14-3-3 from ASK1 with resultant ASK1 kinase activation (6). ASK1 activates both the p38 mitogen-activated protein kinase (MAPK) and the c-*jun* NH_2-terminal kinase (JNK) cascades. In addition, 14-3-3 proteins antagonize apoptosis by binding to the BH3 domain-containing protein BAD and the proapoptotic Forkhead transcription factor FoxO3a/FKHRL1 (1, 24). JNK activation antagonizes 14-3-3 in the regulation of cell survival in at least two ways: first, via phosphorylation of BAD at Ser-128, which inhibits its binding to 14-3-3 (4); second, by direct inactivation of 14-3-3 proteins by phosphorylation of Ser-184 of 14-3-3ζ, Ser-186 of 14-3-3β, and Ser-184 of 14-3-3σ (20).

All seven 14-3-3 family members are expressed in heart tissue, but our results with frog embryos encouraged us to determine whether specific knockdown of one family member, 14-3-3τ, might sensitize tissues to apoptotic stimuli. In this work we investigated mice with targeted disruption of the 14-3-3τ gene.

MATERIALS AND METHODS

Targeted disruption of the 14-3-3τ gene. One allele of the 14-3-3τ gene was disrupted in murine 129/Ola stem cells by BayGenomics (grant U01 HL6662; http://baygenomics.ucsf.edu). In their method, gene trap vectors were electroporated into 129/Ola embryonic stem cells. Rapid-amplification-of-cDNA-ends PCR was used to identify the gene that is likely to be disrupted by the gene trap

* Corresponding author. Mailing address: Center for Cardiovascular Research, Washington University School of Medicine, Box 8086, 660 South Euclid Ave., St. Louis, MO 63110. Phone: (314) 747-3525. Fax: (314) 747-3545. E-mail: amuslin@im.wustl.edu.

▽ Published ahead of print on 4 December 2006.

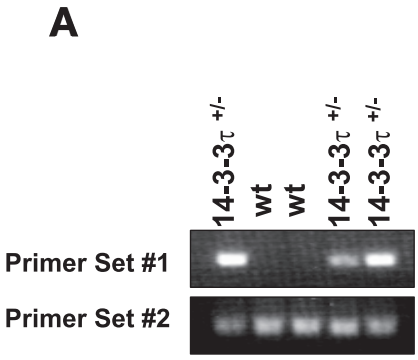

B

	+/+	+/-	-/-
10-11 dpc	5	9	3
12 dpc	8	12	0
13 dpc	2	3	2
14 dpc	1	2	0
15 dpc	2	4	0
16 dpc	7	8	0
19-20 dpc	4	12	0
2 months	45	87	0

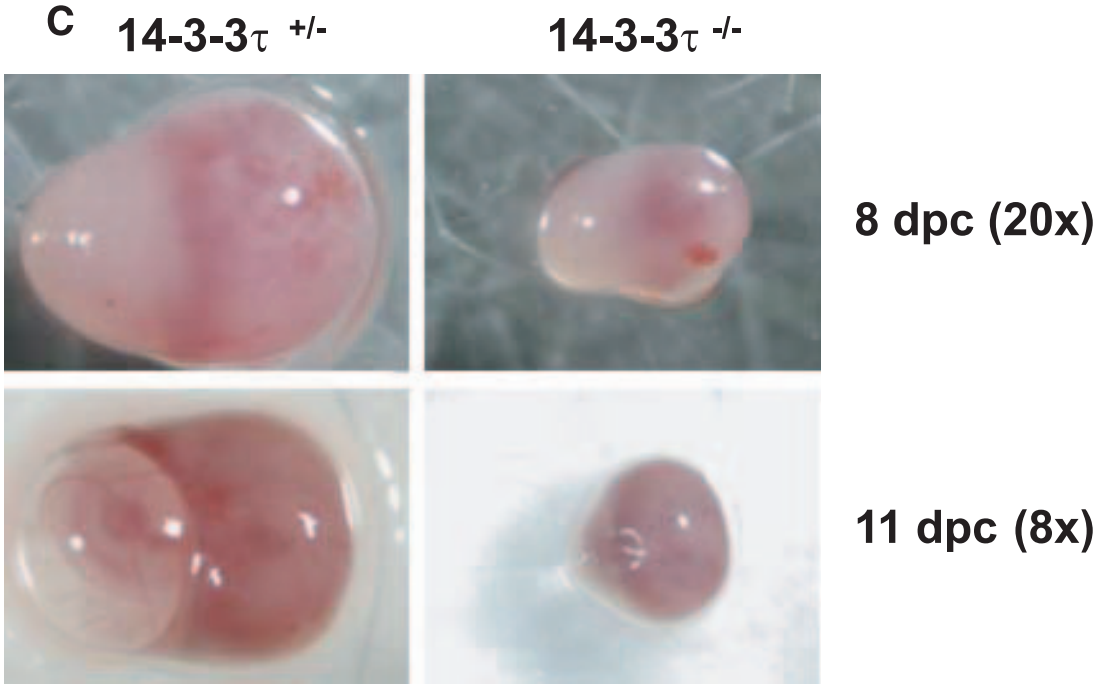

FIG. 1. 14-3-3$\tau^{-/-}$ animals do not survive embryonic development. A. Male and female 14-3-3$\tau^{+/-}$ animals were mated, and embryonic offspring were analyzed for genotype by PCR at specific time points after fertilization. B. 14-3-3$\tau^{-/-}$ embryos die by embryonic day 14. Genetic analysis of embryos obtained from 14-3-3$\tau^{+/-}$ × 14-3-3$\tau^{+/-}$ matings at various embryonic stages. C. Deciduae containing 14-3-3$\tau^{-/-}$ embryos are smaller than heterozygous deciduae. Deciduae from 14-3-3$\tau^{+/-}$ × 14-3-3$\tau^{+/-}$ matings were isolated from adult females at 8 and 11 dpc. In several cases at 11 or 12 dpc, deciduae containing 14-3-3$\tau^{-/-}$ embryos were partially resorbed or were dead (see bottom right panel). D. 14-3-3$\tau^{-/-}$ embryos are hypomorphic and exhibit developmental delay at 9 and 10 dpc. Embryos were carefully dissected from deciduae and were photographed under a dissecting microscope. Embryos were placed in formalin and were again imaged. E. Cardiac development is delayed but is otherwise normal in 14-3-3$\tau^{-/-}$ embryos. Formalin-fixed embryos were embedded in paraffin, sectioned with a microtome, and stained with hematoxylin and eosin. A transverse section of a paraffin-embedded 9-dpc 14-3-3$\tau^{-/-}$ embryo is depicted in the figure. Am, amnion; En, endocardium; FG, foregut diverticulum; Myo, myocardial layer of ventricle; NF, neural folds.

vector. Genes targeted were entered into the BayGenomics database, and corresponding cell lines were stored at −80°C.

Targeted embryonic stem (ES) cells were thawed and passed for 6 days in ES cell medium in the absence of G418. Blastocysts were flushed from pregnant C57BL/6 females (Jackson Laboratory), expanded for 1 to 2 h in ES cell medium, transferred to a hanging drop chamber, and cooled to 4°C. ES cells were added to the hanging drops, and the blastocysts were injected with enough cells (20 or more) to fill the blastocoele. Injected blastocysts were then transferred to pseudopregnant recipient females (10 to 15 blastocysts/uterine horn). Offspring were bred with C57BL/6 mice, and agouti offspring were bred back into the C57BL/6 genetic background.

Protein analysis. Cytosolic extracts of ventricular tissue or cultured adult murine cardiomyocytes were separated by sodium dodecyl sulfate-polyacrylamide gel electrophoresis (SDS-PAGE), and proteins were electrophoretically transferred to nitrocellulose filters that were blocked with milk, washed, and then incubated with primary antibody. Primary antibodies against 14-3-3τ were obtained from Santa Cruz Biotechnology (sc-732) and Biosource (AHZ0542). Other primary antibodies employed were acquired from Cell Signaling Incorporated: anti-phospho-p38 MAPK (no. 9211), anti-cleaved caspase-3 (no. 9665), anti-phospho-Akt (no. 9275), anti-Akt (no. 9272), anti-phospho-JNK (no. 9251), anti-JNK (no. 9252), anti-phospho-extracellular signal-regulated kinase (ERK) (no. 9101), and anti-ERK1/2 (no. 9102). Fil-

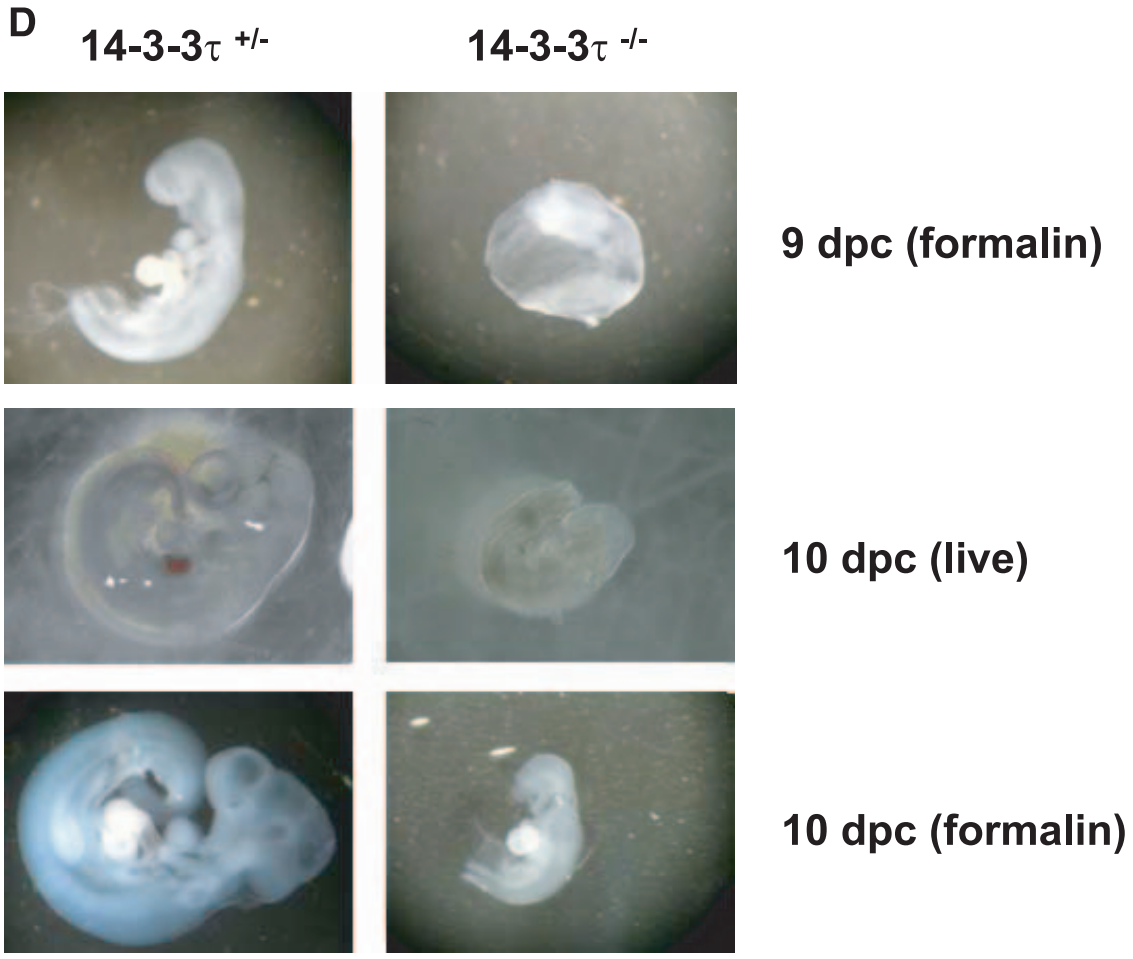

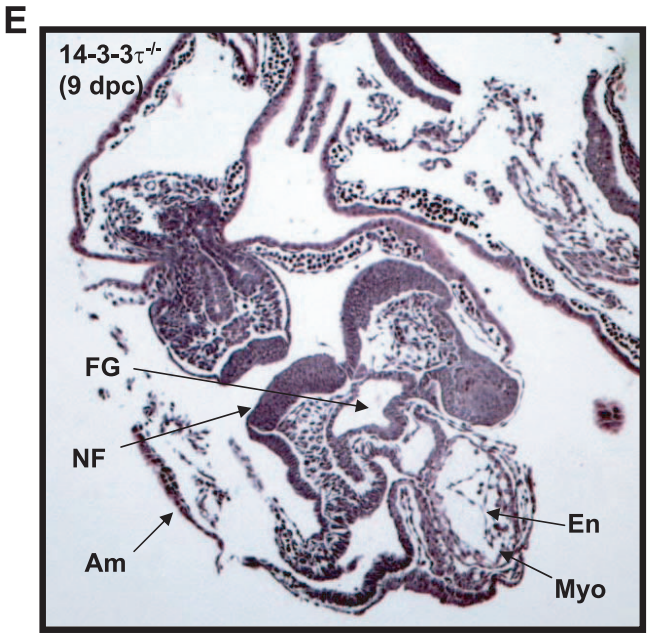

FIG. 1—*Continued.*

ters were extensively washed with 1× Tris-buffered saline–Tween 20 and then were incubated with alkaline phosphatase-conjugated or horseradish peroxidase-conjugated secondary antibodies (Amersham). Bands were visualized with 5-bromo-4-chloro-3-indolylphosphate–Nitro Blue Tetrazolium dissolved in AP buffer or the ECL system (Amersham). Selected bands on scanned immunoblots were quantified by the densitometry computer program Image J (NIH). The target band densities were normalized to the amount of protein loaded in each lane (i.e., total ERK).

TABLE 1. Echocardiographic analysis of wild-type and 14-3-3$\tau^{+/-}$ mice[a]

Genotype (n[b])	HR (min^{-1})	LVIDd (mm)	(LVIDs) (mm)	LVPWd (mm)	IVSd (mm)	LVM (mg)	BW (g)	FS (%)
Wild type (6)	665 ± 46	3.2 ± 0.22	1.32 ± 0.12	0.60 ± 0.07	0.67 ± 0.07	58.2 ± 6.8	22.2 ± 1.1	58.4 ± 2.7
14-3-3$\tau^{+/-}$ (6)	660 ± 11	3.2 ± 0.15	1.12 ± 0.17	0.57 ± 0.10	0.67 ± 0.05	56.0 ± 8.5	21.2 ± 1.5	64.8 ± 5.5

[a] Twelve-week-old awake mice underwent transthoracic echocardiography. HR, heart rate; LVIDd, left ventricular internal dimension in diastole; LVIDs, left ventricular internal dimension in systole; LVPWd, left ventricular posterior wall thickness in diastole; IVSd, interventricular septal thickness in diastole; LVM, calculated left ventricular mass; BW, body weight; FS, fractional shortening.
[b] n, number of mice studied.

Adult mouse cardiomyocyte cultures. Primary adult mouse cardiomyocyte cultures were prepared according to published Alliance for Cell Signaling protocols (18). Briefly, 8- to 12-week-old littermates were sacrificed, and their hearts were cannulated on a 16-gauge needle. Collagenase (1 mg/ml) maintained at 37°C was circulated through the coronary arterial system for ~20 min. Hearts were minced, and dissolved calcium was introduced into the medium. Cardiomyocytes were plated onto laminin-coated tissue culture vessels and serum deprived (minimal essential medium–Hanks' buffered salt solution containing 10 mM 2,3-butanedione monoxime, 0.55 g/ml transferrin, and 0.5 ng/ml selenium) prior to experimentation.

For UVC irradiation studies, after a 4-h or overnight serum deprivation, cells were irradiated with 180 J/m^2 UVC (UV Stratalinker 2400; Stratagene). Irradiated cells were incubated for 12 or 24 h and then harvested. For H_2O_2 stimulation studies, cardiomyocytes were serum starved for 4 to 12 h, treated with 10 μM H_2O_2 for 12 h, and then harvested.

Experimental myocardial infarction. Myocardial infarction surgery was performed as previously described (3, 17). In brief, anesthetized and ventilated 12-week-old mice were subjected to thoracotomy. A single 8-0 prolene suture was tied around the proximal left coronary artery (17). Successful occlusion was confirmed by the appearance of pallor of the anterior wall of the left ventricle. The incision was closed, and the animal was allowed to recover on a heating pad. The surgeon was blinded to the genotype of the mice in every case. After 1 or 7 days, animals were subjected to transthoracic echocardiography. After 7 days, animals were killed and the hearts were dissected and weighed.

Treatment of mice with SB202190. Mice between 8 and 12 weeks old were injected with SB202190, a p38 MAPK inhibitor, at a dose of 5 mg/kg of body weight/day. SB202190 was dissolved in 50% dimethyl sulfoxide with water. Control vehicle injection was performed by injection of a 50% dimethyl sulfoxide water solution. On day 4 of SB202190 injection, mice were subjected to myocardial infarction by the method described above. Survival was recorded for the next 5 days. After 5 days the mice were euthanized, and hearts were excised for histological analysis.

Transthoracic echocardiography. Transthoracic echocardiography was performed with mice that were awake by use of the Acuson Sequoia 256 echocardiography system equipped with a 15-MHz (15L8) transducer as described previously (Acuson) (17). The echocardiographer was blinded in all cases to the genotype of the mice.

Histological analysis. Murine embryos or adult hearts were fixed in 10% formalin in phosphate-buffered saline, embedded in paraffin, and sectioned with a microtome. Hematoxylin and eosin or Masson's trichrome was used to stain paraffin sections.

TUNEL. Animals were euthanized, and hearts were excised and fixed overnight at room temperature in 10% formalin in phosphate-buffered saline, embedded in paraffin, and sectioned with a microtome. The terminal deoxynucleotidyltransferase nicked-end labeling (TUNEL) assay was performed on 10-μm sections (TdT-FragEL DNA fragmentation detection kit; Oncogene, Cambridge, MA). Sections were mounted on coverslips by Permount (Fisher) and evaluated by colorimetric or fluorescence microscopy.

Analysis of murine embryos. Embryos were isolated from pregnant females by the method described by Liu et al. (9). Cages were set up with 14-3-3$\tau^{+/-}$ × 14-3-3$\tau^{+/-}$ mating pairs. Pregnant mice were euthanized by CO_2 asphyxiation at various times after mating. Entire conceptuses and placentae were isolated between 7 days postcoitum (dpc) and 17 dpc from pregnant females and photographed. A portion of the yolk sac or embryo was used to generate chromosomal DNA for genotyping by PCR. The embryos and placentae were fixed in 10% formalin in phosphate-buffered saline for histological analyses.

Statistical analysis. All data are reported as means ± standard errors of the means. Statistical analysis was performed by a two-tailed Student t test, analysis of variance, and the Kaplan-Meier log-rank test, where applicable. A P value of <0.05 was considered to be statistically significant.

RESULTS

Targeted disruption of 14-3-3τ. Inspection of the Bay Genomics web site (http://baygenomics.ucsf.edu) revealed that a murine embryonic 129/Ola stem cell line had been generated with disruption of the 14-3-3τ genomic locus. This cell line was subsequently expanded, and targeted stem cells were injected into C57Bl/6J blastocysts and then placed in pseudopregnant females. Chimeric offspring were bred with C57BL/6J mice, and this demonstrated that germ line transmission had occurred in one chimeric mouse. Insertion of the gene trap vector into the 14-3-3τ gene was confirmed by DNA sequencing of a PCR product derived from murine genomic DNA (data not shown).

Interbreeding of 14-3-3$\tau^{+/-}$ offspring was performed, but live-born 14-3-3$\tau^{-/-}$ mice were never identified by tail-preparation DNA PCR analysis (Fig. 1A). To determine the stage at which 14-3-3$\tau^{-/-}$ embryos died, embryos from heterozygote breeding pairs were obtained at various gestational ages. DNA was obtained from embryos and used for PCR to determine the genotype of each embryo. PCR analysis revealed that knockout embryos were present at near-Mendelian ratios at 10 dpc but not at 14 dpc. These experiments demonstrated that most knockout embryos died between 12 dpc and 13 dpc (Fig. 1B).

Examination of 8- to 11-dpc embryos demonstrated that 14-3-3$\tau^{-/-}$ embryos exhibited signs of developmental arrest, with smaller deciduae in many cases, similar to heterozygous

TABLE 2. Invasive analysis of cardiac physiology in wild-type and 14-3-3$\tau^{+/-}$ mice[a]

Genotype (n[b])	HR (min^{-1})	LVP_{max} (mm Hg)	LVP_{ed} (mm Hg)	dP/dt_{max} (mm Hg/s)	dP/dt_{min} (mm Hg/s)	Tau (Weiss) (ms)
Wild type (5)	534 ± 18	93 ± 12	5.0 ± 0.8	7,092 ± 2,529	−7,644 ± 2,021	8.0 ± 0.8
14-3-3$\tau^{+/-}$ (5)	551 ± 37	94 ± 11	6.0 ± 2.0	6,209 ± 1,283	−7,159 ± 1,606	9.0 ± 1.9

[a] Twelve-week-old anesthetized mice underwent invasive cardiac catheterization. HR, heart rate; LVP_{max}, left ventricular peak systolic pressure; LVP_{ed}, left ventricular end-diastolic pressure; dP/dt_{max}, maximal change in pressure per unit of time; dP/dt_{min}, minimal change in pressure per unit of time; Tau, calculated index of diastolic function.
[b] n, number of mice studied.

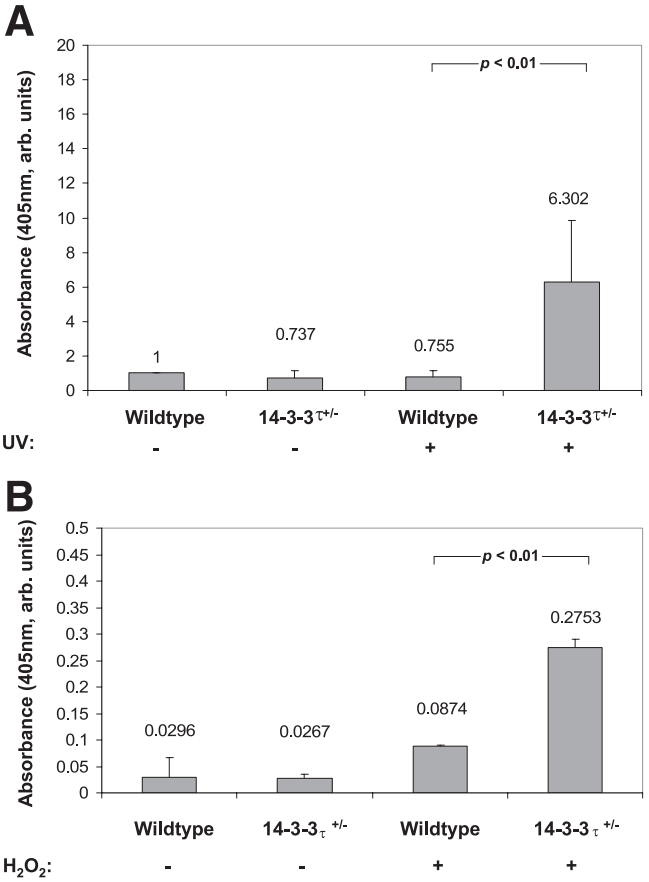

FIG. 2. Increased apoptosis in adult murine cardiomyocytes obtained from 14-3-3$\tau^{+/-}$ mice. A. Adult cardiomyocytes were isolated from 14-3-3$\tau^{+/-}$ and wild-type 10- to 12-week-old mice and treated with UVC irradiation (180 J/m^2), a well-described stimulus of apoptosis. 14-3-3$\tau^{+/-}$ cardiomyocytes displayed an approximately eightfold-higher rate of apoptosis than wild-type cells in response to UVC irradiation (6.30% ± 3.50% for 14-3-3$\tau^{+/-}$ mice versus 0.76% ± 0.37% for wild-type mice; $P < 0.05$; see Fig. 4A). B. 14-3-3$\tau^{+/-}$ cardiomyocytes were also sensitized to H_2O_2-induced apoptosis. Treatment of cells with 10 μM of H_2O_2 for 12 h caused 14-3-3$\tau^{+/-}$ cardiomyocytes to undergo apoptosis at an approximately 3.5-fold-higher rate than wild-type cardiomyocytes (0.2753% ± 0.0154% for 14-3-3$\tau^{+/-}$ mice versus 0.0874% ± 0.002% for wild-type mice; $P < 0.05$; see Fig. 4B). arb. units, arbitrary units.

embryos at earlier stages, especially at 8 dpc (Fig. 1C). Dissection of deciduae revealed that occasional 14-3-3$\tau^{-/-}$ embryos were undergoing resorption at 8 to 11 dpc, while others were developmentally delayed and hypomorphic (Fig. 1C and D). Gross inspection and histologic examination of 14-3-3$\tau^{-/-}$ and heterozygous embryos at these developmental stages revealed generalized developmental delay, without specific defects noted in the cardiovascular system (Fig. 1D and E).

To confirm that 14-3-3$\tau^{-/-}$ embryos lacked 14-3-3τ mRNA, we performed a quantitative real-time reverse transcription-PCR analysis of 9-dpc embryos with primers specific for 14-3-3τ. This analysis revealed that 14-3-3$\tau^{-/-}$ embryos contained minimal, if any, mRNA encoding 14-3-3τ (data not shown).

Evaluation of cardiac function in adult 14-3-3$\tau^{+/-}$ mice. Although 14-3-3$\tau^{-/-}$ mice did not survive embryonic development, 14-3-3$\tau^{+/-}$ mice appeared grossly normal at birth and were fertile. The body weights of 14-3-3$\tau^{+/-}$ mice were similar to those of wild-type (WT) littermates measured at 6, 8, 10, and 12 weeks after birth (data not shown). We evaluated whether 14-3-3τ mRNA and protein levels were reduced in haploinsufficient mice. We found that these mice had an approximately 50% reduction in 14-3-3τ protein in cardiac tissue samples (data not shown). Reverse transcription-PCR analysis also showed that there was a reduction of approximately 50% in 14-3-3τ mRNA expression in 14-3-3$\tau^{+/-}$ mice (data not shown). The mRNA levels for all other 14-3-3 family members, including 14-3-3β, 14-3-3ε, 14-3-3γ, 14-3-3η, 14-3-3σ, and 14-3-3ζ, were tested in cardiac tissue obtained from 14-3-3$\tau^{+/-}$ mice. The mRNA levels of these family members were unchanged in 14-3-3$\tau^{+/-}$ cardiac tissue (data not shown).

We examined cardiac physiology in adult 14-3-3$\tau^{+/-}$ mice to determine whether knock-down of 14-3-3τ protein would sensitize cardiomyocytes to proapoptotic stimuli. Next, we evaluated the basal cardiac structure and function in 12-week-old 14-3-3$\tau^{+/-}$ mice. Echocardiography demonstrated that 14-3-3$\tau^{+/-}$ mice had normal systolic function and normal cardiac chamber sizes and mass (Table 1). Morphometric and histologic analyses showed that the left-ventricular-weight-to-body-weight ratio and cardiomyocyte cell size (measured by cross-sectional area on left ventricular tissue sections) were similar between 14-3-3$\tau^{+/-}$ mice and wild-type littermates (data not shown). Cardiac catheterization of 12-week-old 14-3-3$\tau^{+/-}$ mice showed that the 14-3-3$\tau^{+/-}$ mice hearts had hemodynamic properties similar to those of wild-type littermates (Table 2).

Increased apoptosis in cultured adult 14-3-3$\tau^{+/-}$ cardiomyocytes. We previously demonstrated that a primary role of mammalian 14-3-3 proteins is to prevent cell death by apoptosis (22). To determine whether reduction of the 14-3-3τ protein would sensitize cardiomyocytes to proapoptotic stimuli, we isolated and cultured adult cardiomyocytes from 14-3-3$\tau^{+/-}$ and wild-type 10- to 12-week-old littermates and treated the cells with UVC irradiation (180 J/m^2), a well-described stimulus of apoptosis. 14-3-3$\tau^{+/-}$ cardiomyocytes displayed an approximately eightfold

TABLE 3. Echocardiographic analysis of wild-type and 14-3-3$\tau^{+/-}$ mice after myocardial infarction[a,b]

Genotype (n[c])	SWMSI (1 day)	EDV (7 days) (mm^3)	EDVI (7 days) (mg)	ESV (7 days) (mm^3)	EF (7 days)
Wild type (12)	1.40 ± 0.03	70.7 ± 7.2	3.05 ± 0.41	47.3 ± 7.7	38.1 ± 5.4
14-3-3$\tau^{+/-}$ (11)	1.37 ± 0.03	105.1 ± 12.3	3.80 ± 0.40	78.9 ± 11.7	28.3 ± 3.2

[a] Twelve-week-old awake mice underwent transthoracic echocardiography 1 or 7 days after experimental myocardial infarction by ligation of the left coronary artery. SWMSI, segmental wall motion score index (an SWMSI value of 1 indicates normal wall thickening, whereas an SWMSI score of 2 indicates cardiac akinesis). EDV, end diastolic volume; EDVI, end diastolic volume index (end diastolic volume/body weight in mg); ESV, end systolic volume (mm^3); EF, ejection fraction.

[b] P values were as follows: for SWMSI, 0.37; for EDV, 0.022; for EDVI, 0.20; for ESV, 0.03; for EF, 0.14.

[c] n, number of mice studied.

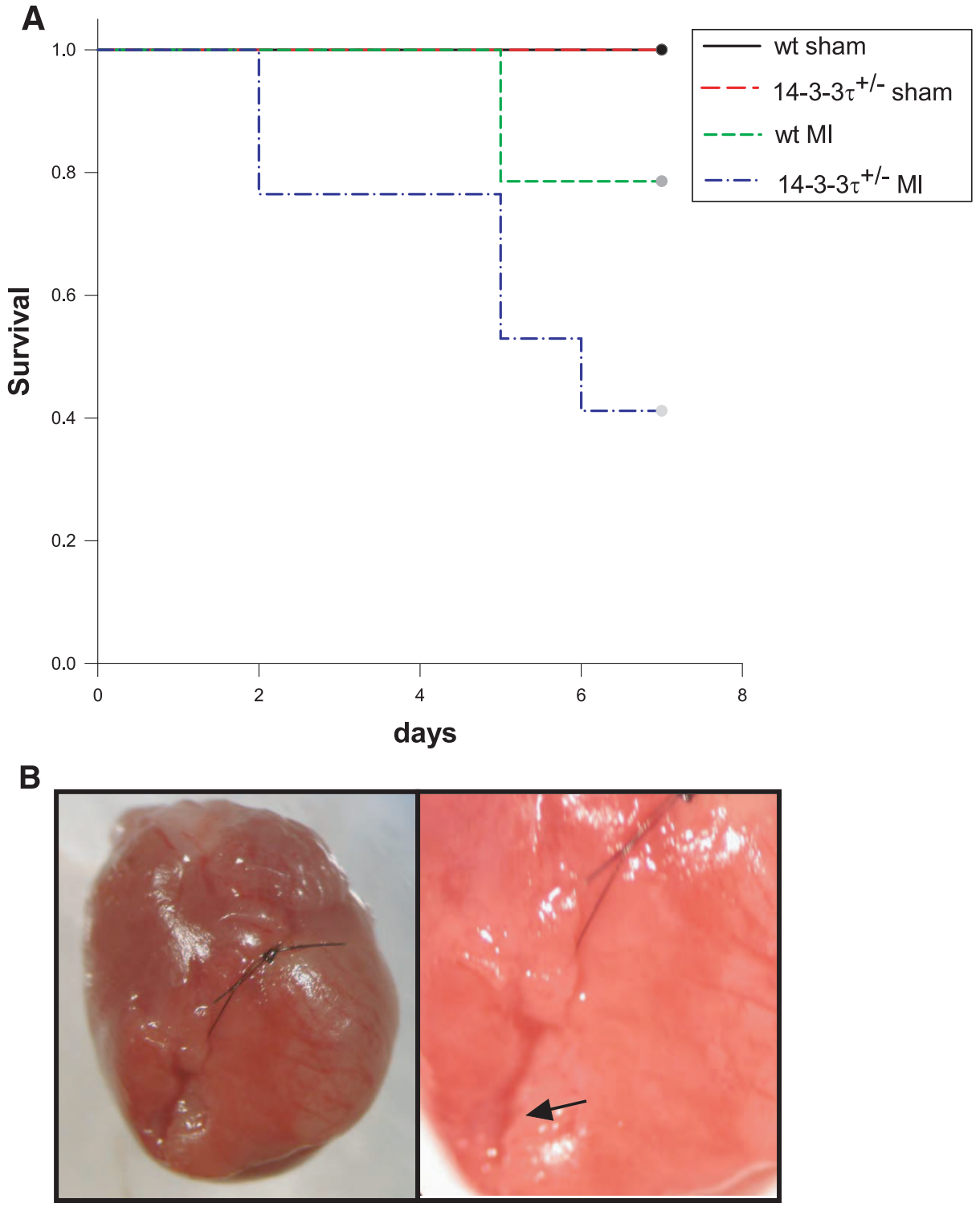

FIG. 3. Increased cardiac remodeling after myocardial infarction in 14-3-3$\tau^{+/-}$ mice. A. Kaplan-Meier survival analysis after myocardial infarction. 14-3-3$\tau^{+/-}$ mice had much higher mortality 7 days following left coronary artery ligation. B. Ventricular free wall rupture occurs in 14-3-3$\tau^{+/-}$ mice following myocardial infarction surgery. Hearts were isolated from mice and viewed with a dissecting microscope. The right panel depicts a close-up view of the site of rupture (arrow) in the same heart shown in the left panel. C. Histologic analysis of infarct size 7 days after ligation of the left coronary artery in wild-type and 14-3-3$\tau^{+/-}$ mice. Hearts were isolated, fixed in formalin, embedded in paraffin, sectioned with a microtome, stained with trichrome, and analyzed by computerized microscopy. D. Quantitative analysis of histological sections described for panel B. The area of infarction was divided by the total left ventricular area in each section. Ten sections per heart were analyzed. E. Analysis of cardiomyocyte apoptosis in the infarct border zone by TUNEL. Hearts were isolated 7 days after myocardial infarction, fixed in formalin, embedded in paraffin, sectioned with a microtome, and analyzed by TUNEL. The infarct border zone was defined as one-quarter circumference of the left ventricle on either side of the infarct. F. Analysis of caspase-3 activation in ventricular tissue after myocardial infarction. Ventricles were isolated 7 days after myocardial infarction, minced, and used to obtain protein lysates. Protein lysates were separated by SDS-PAGE and analyzed by immunoblotting for cleaved caspase-3. Blots were reprobed for total Akt to control for loading.

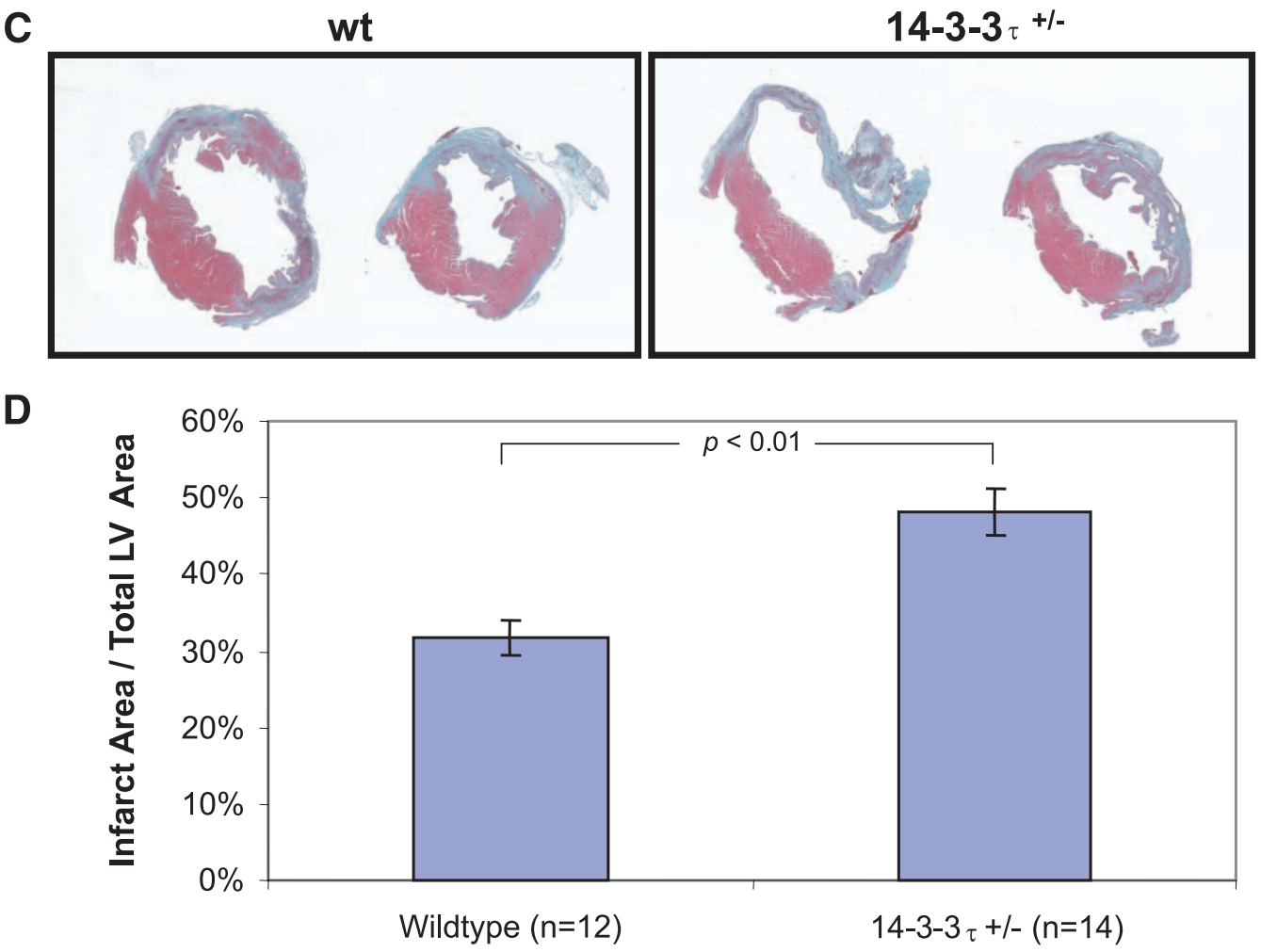

FIG. 3—*Continued.*

higher rate of apoptosis than wild-type cells in response to UVC irradiation (6.30% ± 3.50% for 14-3-3$\tau^{+/-}$ mice versus 0.76% ± 0.37% for WT mice; $P < 0.05$) (Fig. 2A). We next determined whether 14-3-3$\tau^{+/-}$ cardiomyocytes were sensitized to additional factors known to promote apoptosis. Treatment of cells with 10 μM of H_2O_2 for 12 h caused 14-3-3$\tau^{+/-}$ cardiomyocytes to undergo apoptosis at an approximately 3.5-fold higher rate than wild-type cardiomyocytes (0.2753% ± 0.0154% for 14-3-3$\tau^{+/-}$ cardiomyocytes versus 0.0874% ± 0.002% for the WT; $P < 0.05$) (Fig. 2B).

Increased pathological remodeling after myocardial infarction in 14-3-3$\tau^{+/-}$ mice. Since 14-3-3$\tau^{+/-}$ cardiomyocytes were sensitized to proapoptotic stimuli, we hypothesized that 14-3-3$\tau^{+/-}$ mice would exhibit increased pathological cardiac remodeling after experimental myocardial infarction surgery. In response to coronary artery ligation, there is an initial infarction stage characterized by widespread necrosis and to a lesser extent apoptosis in the myocardium directly supplied by the occluded vessel. In the days and weeks after a myocardial infarction, a chronic phase of ventricular remodeling occurs that is often maladaptive and that is characterized by persistent cardiomyocyte apoptosis, thinning of the ventricular wall at the infarct site, fibrosis, chamber enlargement, and cardiac myocyte hypertrophy (17).

Experimental myocardial infarction was performed on 14-3-3$\tau^{+/-}$ and wild-type littermates by a surgeon who was blinded to the genotypes of the mice. Coronary artery anatomy is variable in mice; therefore, the area of myocardium affected by coronary artery ligation was quantified in every animal on the day after surgery. Once a murine coronary artery is ligated, myocardium supplied by that artery exhibits reduced or absent contractile function. Quantitative two-dimensional echocardiography was performed 1 day after surgery to determine the segmental wall motion score index (SWMSI), and this demonstrated that the area of myocardium directly supplied by the ligated coronary arteries was nearly identical in wild-type and 14-3-3$\tau^{+/-}$ mice. An SWMSI value of 1 indicates normal wall thickening, whereas an SWMSI score of 2 indicates absent ventricular wall motion (akinesis). The initial SWMSI was 1.40 ± 0.03 for wild-type mice and was 1.37 ± 0.03 for 14-3-3$\tau^{+/-}$ mice (*P* value not significant) (Table 3).

Although all animals survived for the first 24 h after experimental myocardial infarction surgery, the mortality rate was higher for 14-3-3$\tau^{+/-}$ mice over the following 6 days. Eleven out

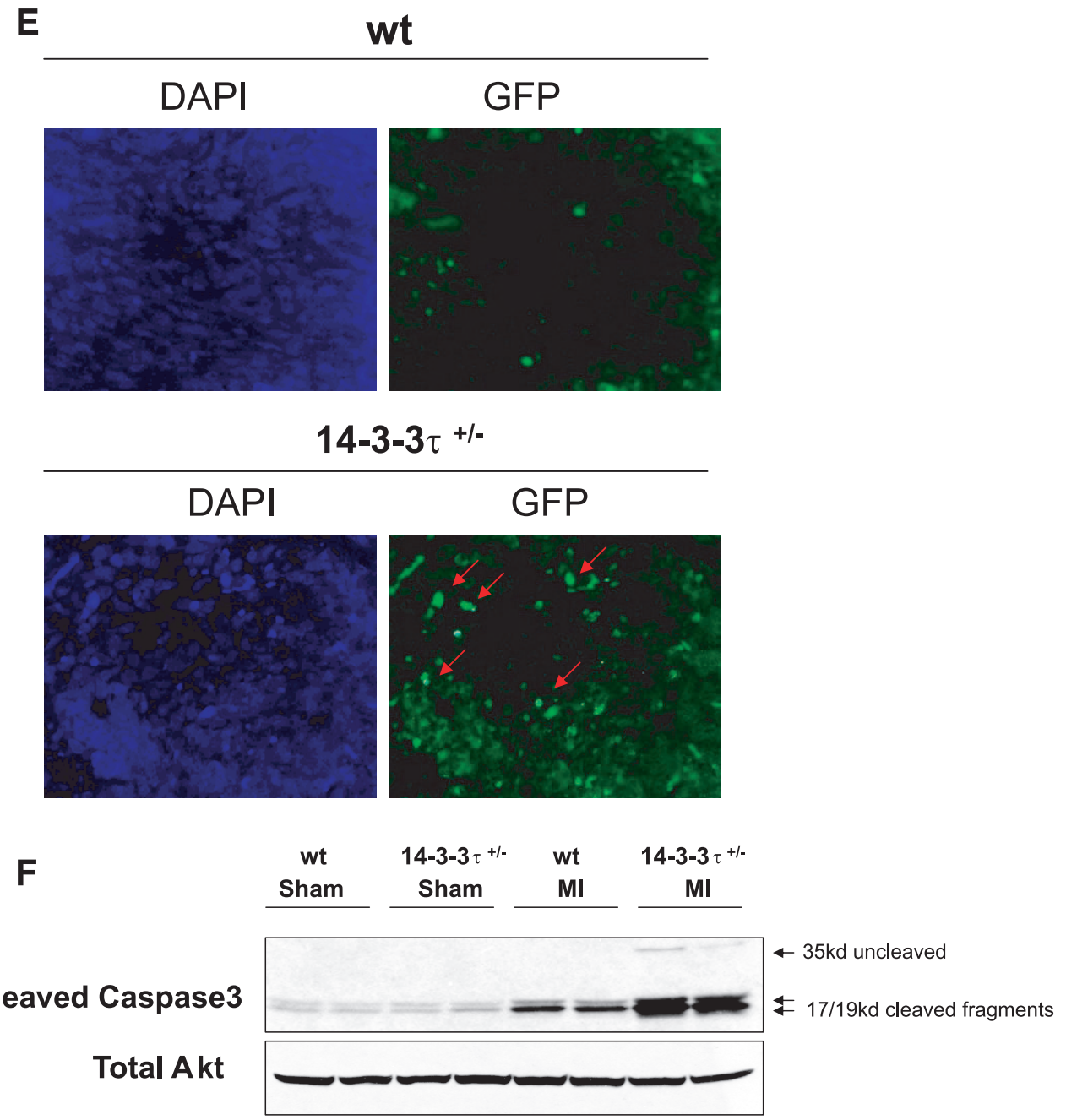

FIG. 3—*Continued.*

of fifteen wild-type animals (73%) survived for at least 7 days after myocardial infarction surgery (Fig. 3A). In contrast, only 7 out of 17 14-3-3$\tau^{+/-}$ mice (41%) were alive 7 days after surgery (Fig. 3A). This difference in survival was statistically significant by log-rank test ($\chi^2 = 4.8236$; $P < 0.05$). Analysis of deceased mice by necropsy revealed that mice uniformly died from ventricular free wall rupture (Fig. 3B). To exclude the possibility that 14-3-3$\tau^{+/-}$ mice were uniquely sensitive to anesthesia or thoracotomy, sham operations were performed, and all 14-3-3$\tau^{+/-}$ mice tolerated the sham procedure and survived for 7 days.

To evaluate ventricular remodeling after myocardial infarction, echocardiography was performed 1 week after myocardial infarction surgery with surviving mice (Table 3). 14-3-3$\tau^{+/-}$ mice exhibited marked left ventricular dilatation compared to wild-type mice. End systolic volume and end diastolic volume were significantly higher in 14-3-3$\tau^{+/-}$ mice than in wild-type animals ($P < 0.05$ for both ESV and EDV) (Table 3). The left ventricular ejection fraction was reduced in 14-3-3$\tau^{+/-}$ heart, but this reduction was not statistically significant (Table 3).

To further evaluate the remodeling process in ventricular tissue, the size of infarcted myocardium was evaluated 7 days after left coronary artery ligation. The size of the myocardial

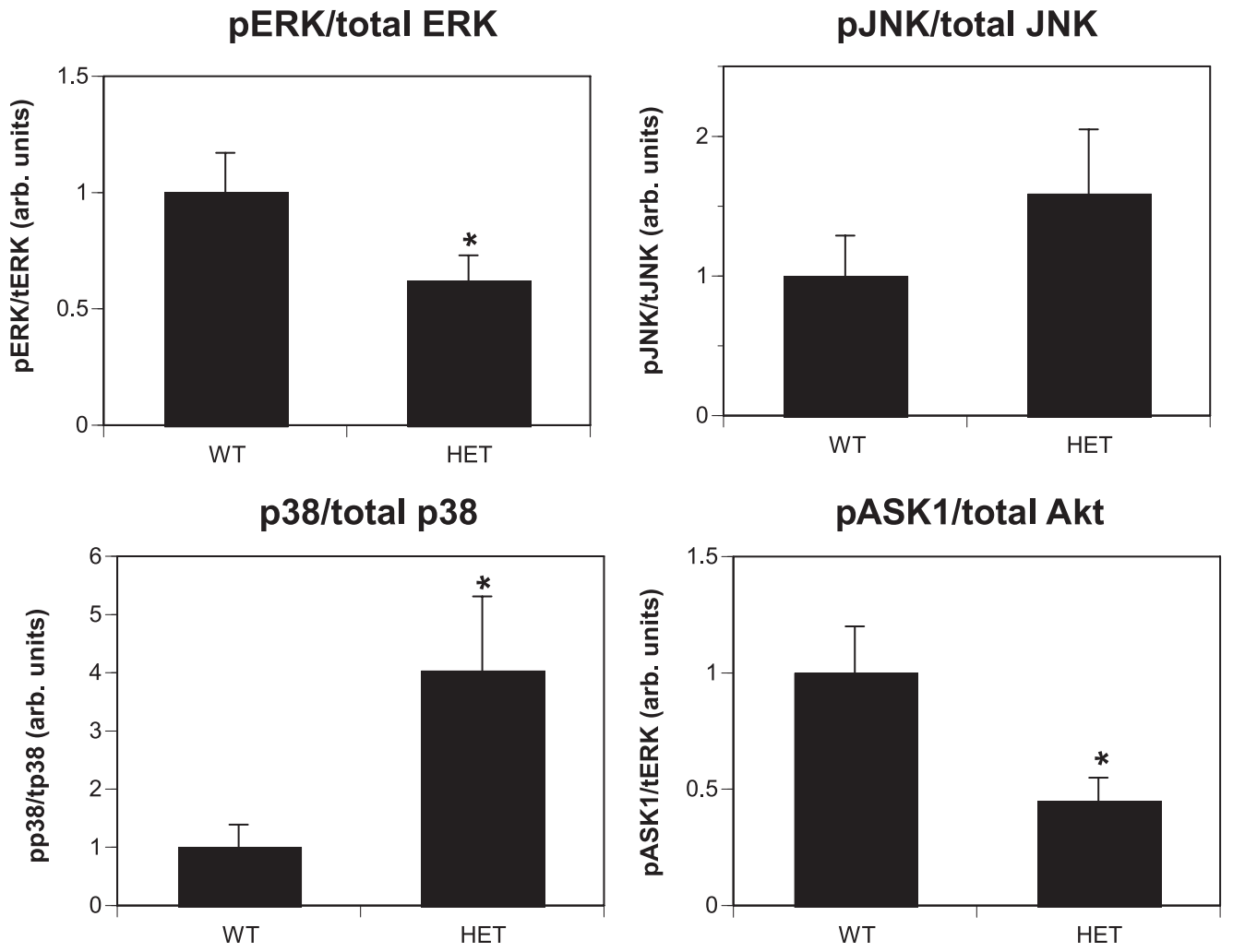

FIG. 4. Analysis of signaling protein activity in 14-3-3$\tau^{+/-}$ mice. Protein lysates were generated from ventricular tissue obtained from 10- to 12-week-old wild-type and 14-3-3$\tau^{+/-}$ mice. Lysates were separated by SDS-PAGE and analyzed by immunoblotting with primary antibodies directed against phosphorylated p38, phosphorylated JNK, total JNK, phosphorylated ERK MAPK, total ERK MAPK, phosphorylated ASK1, phosphorylated Akt, and total Akt. Immunoblots were quantified by the computerized densitometry program Image J (NIH). Results were combined from three separate experiments ($n = 11$ for the wild type; $n = 11$ for 14-3-3$\tau^{+/-}$ mice). arb. units, arbitrary units.

infarction at this time point reflects both the initial infarct size and infarct expansion that occurs with pathological remodeling. Hearts were isolated 7 days after left coronary artery ligation, fixed in 10% formalin, embedded in paraffin, and sectioned with a microtome. Histological examination of trichrome-stained ventricular tissue sections revealed that the area of myocardial infarction was significantly greater in 14-3-3$\tau^{+/-}$ mice than in wild-type animals (48.0% ± 3.1% versus 31.9% ± 2.3%; $P < 0.005$) (Fig. 3C and D).

Apoptosis in the infarct border zones is a hallmark of pathological ventricular remodeling after myocardial infarction. Evaluation of apoptosis in the infarct border zones by TUNEL revealed that there were significantly more TUNEL-positive nuclei in 14-3-3$\tau^{+/-}$ than in wild-type ventricular tissue (Fig. 3E). In a separate set of experiments, left ventricular tissue obtained 7 days after myocardial infarction surgery was used to generate protein lysates. Immunoblotting with an anti-cleaved caspase-3 antibody showed greatly increased cleaved caspase-3 protein levels in 14-3-3$\tau^{+/-}$ ventricular tissue than in wild-type ventricular tissue (Fig. 3F).

Altered signal transduction in 14-3-3$\tau^{+/-}$ cardiac tissue. We previously demonstrated that global inhibition of 14-3-3 proteins in cardiac tissue by overexpression of a dominant-negative form of 14-3-3η resulted in increased ASK1, p38 MAPK, and JNK activity (22). To determine whether selective knock-down of 14-3-3$\tau^{+/-}$ would also result in increased cardiac ASK1 signaling, a series of signal transduction experiments was performed.

Activation of ASK1 was evaluated by immunoblotting with an antibody that recognizes the inactive (Ser-84-phosphorylated) form of this protein, and this revealed that ASK1 activation was higher in 14-3-3$\tau^{+/-}$ ventricular tissue (Fig. 4). Activation of JNK and p38 MAPK was evaluated by immunoblotting with antibodies that specifically recognize the active (phosphorylated) forms of these proteins. Analysis of ventricular protein lysates obtained from 12-week-old mice revealed

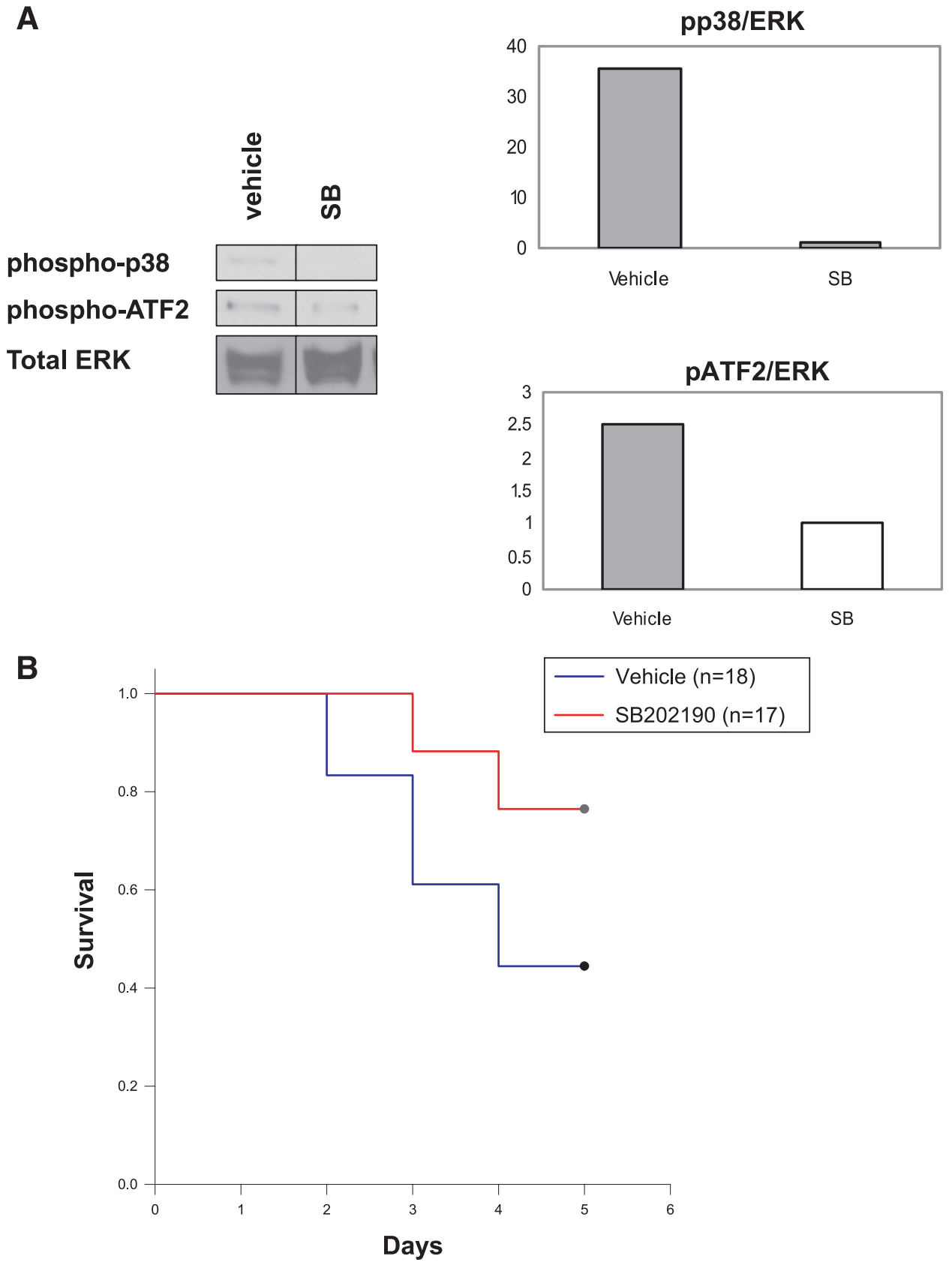
A
vehicle
SB
phospho-p38
phospho-ATF2
Total ERK
pp38/ERK
40
30
20
10
0
Vehicle
SB
pATF2/ERK
3
2.5
2
1.5
1
0.5
0
Vehicle
SB
B
Vehicle (n=18)
SB202190 (n=17)
Survival
1.0
0.8
0.6
0.4
0.2
0.0
0
1
2
3
4
5
6
Days

that there was increased activation of JNK and p38 MAPK in 14-3-3$\tau^{+/-}$ tissue compared to wild-type tissue (Fig. 4). In contrast, ERK MAPK activation was reduced in 14-3-3$\tau^{+/-}$ ventricular tissue compared to wild-type tissue (Fig. 4). Results shown in Fig. 4 were combined from three separate experiments ($n = 11$ for the wild type; $n = 11$ for 14-3-3$\tau^{+/-}$ mice).

Inhibition of p38 MAPK improved survival for 14-3-3$\tau^{+/-}$ mice after myocardial infarction. We previously demonstrated that pharmacologic or genetic inhibition of p38α MAPK activity in heart tissue ameliorated the proapoptotic phenotype observed in DN-14-3-3η transgenic mice (26). To determine whether the increased apoptosis observed in 14-3-3$\tau^{+/-}$ cardiomyocytes was due to increased p38 MAPK activity, we treated wild-type and 14-3-3$\tau^{+/-}$ mice with SB202190, a p38α and -β inhibitor, by intraperitoneal injection (5 mg/kg/day). Left coronary artery ligation was performed after 3 days of SB202190 administration. Mice were monitored for survival until the eighth day of SB202190 treatment.

To confirm that SB202190 effectively blocked p38 MAPK activity, cardiac protein lysates were generated after 8 days of treatment. Cardiac protein lysates were analyzed by anti-phospho-p38 MAPK and by anti-phospho-activity transcription factor 2 (ATF2) immunoblotting. ATF2 is a well-defined substrate for p38 MAPK. Phosphorylation of p38 MAPK and ATF2 was markedly reduced in the myocardium of SB202190-treated 14-3-3$\tau^{+/-}$ mice compared to results with vehicle-treated 14-3-3$\tau^{+/-}$ mice (Fig. 5A).

Vehicle-treated 14-3-3$\tau^{+/-}$ mice had a survival rate of only 47% after myocardial infarction (8/17 animals survived) (Fig. 5B). In contrast, injection of 14-3-3$\tau^{+/-}$ mice with SB202190 increased the survival rate to 76% (13/17 survived), which is similar to the rate observed with wild-type mice after myocardial infarction. This difference in survival was statistically significant by log-rank test ($\chi^2 = 4.175$; $P < 0.05$). Therefore, pharmacological inhibition of p38 MAPK reversed the enhanced mortality of 14-3-3$\tau^{+/-}$ mice after myocardial infarction.

DISCUSSION

The 14-3-3 family regulates many aspects of cell physiology, but the antiapoptotic effect of these proteins may be of primary import. Previous work demonstrated that global inhibition of 14-3-3 action by use of peptide inhibitors or dominant-negative mutant forms of 14-3-3 proteins sensitized cultured cells and cardiac tissue to proapoptotic stimuli (11, 22). However, a specific requirement for a particular family member was not established. In the current work, the 14-3-3τ genomic locus was disrupted and mice haploinsufficient for 14-3-3τ were examined. 14-3-3$\tau^{-/-}$ mice did not survive embryonic development, and all embryos died by 14 dpc. 14-3-3$\tau^{-/-}$ embryos were hypomorphic and exhibited developmental delay compared to heterozygous embryos at 8 to 11 dpc. In contrast, haploinsufficient mice appeared normal at birth, but cultured cardiomyocytes from haploinsufficient mice were sensitized to proapoptotic stimuli. Furthermore, 14-3-3$\tau^{+/-}$ mice developed larger myocardial infarctions with exaggerated pathological cardiac remodeling after occlusion of the left coronary artery. These results demonstrate that 14-3-3τ plays an important antiapoptotic role in cardiac tissue. The current work is the first to show a specific requirement for an individual 14-3-3 family member in cell survival.

The mechanisms underlying the antiapoptotic effect of 14-3-3τ in cardiac tissue are not completely understood, but our data suggest that the ASK1-p38 MAPK signaling pathway is involved in this biologic effect. The protein kinase ASK1 is thought to be a powerful mediator of apoptosis in cardiac tissue in response to various types of external stress. In 14-3-3τ cardiac tissue, ASK1 and its downstream effectors p38 MAPK and JNK exhibited increased activation in comparison to results with wild-type cardiac tissue. Pharmacologic inhibition of p38 MAPK in 14-3-3$\tau^{+/-}$ mice ameliorated the proapoptotic phenotype observed after experimental myocardial infarction. Experiments are ongoing to determine whether direct inhibition of ASK1 or JNK activity can also reverse the cardiac phenotype in 14-3-3$\tau^{+/-}$ mice.

Many studies have shown that pharmacologic or genetic inhibition of p38α/β MAPK reduced cardiomyocyte apoptosis in response to provocative stimuli in rodents (8, 10, 16, 17, 19, 26). Paradoxically, cardiac-specific ablation of p38α MAPK in mice also promoted cardiomyocyte apoptosis in response to pressure overload by transverse aortic constriction (15). One interpretation of these data is that low-level activity of p38α MAPK promotes cardiomyocyte survival, perhaps indirectly through expression of additional proteins, but that activation above a particular threshold is proapoptotic. Given that there is evidence of low-level p38α MAPK activation in apparently healthy cardiomyocytes, this may be a reasonable hypothesis. The mechanisms by which p38 MAPK promotes cardiomyocyte apoptosis may include the ability of p38 MAPK to induce the deamidation of BCL-X(L) (17). In addition, p38 MAPK enhances the phosphorylation and activation of the proapoptotic transcription factor p53 (2).

14-3-3τ likely inhibits apoptosis through a variety of mechanisms in addition to its ability to antagonize ASK1 signaling, and the ability of 14-3-3τ to sequester BAD and FOXO family members may also be important for this effect. Previous work demonstrated that the treatment of rat neonatal cardiomyocytes with phenylephrine promoted the phosphorylation and inactivation of BAD via binding to 14-3-3 (21). It is likely that

FIG. 5. Reduced mortality after myocardial infarction in response to p38 MAPK inhibition. SB202190, a p38α and -β inhibitor, was injected intraperitoneally into wild-type and 14-3-3$\tau^{+/-}$ animals (5 mg/kg/day). A. Reduced cardiac p38 MAPK activity in 14-3-3$\tau^{+/-}$ mice injected with SB202190. Protein lysates were generated from hearts taken from mice injected daily with SB202190 (SB) or vehicle for 8 days. Cardiac lysates were analyzed by anti-phospho-p38 MAPK and anti-phospho-ATF2 immunoblotting. Anti-total-ERK MAPK immunoblotting was performed to control for protein loading. B. SB202190 treatment increases survival for 14-3-3$\tau^{+/-}$ mice after MI. Left coronary artery ligation was performed after 3 days of SB202190 administration. The increased survival of 14-3-3$\tau^{+/-}$ mice injected with SB202190 compared to mice injected with vehicle was statistically significant by the log-rank test (76% versus 46%; $P = 0.046$).

14-3-3τ modulates the activity of multiple enzymatic cascades to ensure the survival of cardiomyocytes.

ACKNOWLEDGMENTS

This work was supported by grants from the National Institutes of Health (HL061567, HL057278, and HL076670) and the Burroughs Wellcome Fund (A.J.M.).

We acknowledge the assistance of the Washington University Mouse Cardiovascular Phenotyping Core and the Digestive Diseases Research Core Center (NIH P30 DK52574). We thank David Ornitz for helpful advice.

REFERENCES

1. **Brunet, A., A. Bonni, M. J. Zigmond, P. Juo, L. S. Hu, M. J. Anderson, K. C. Arden, J. Blenis, and M. E. Greenberg.** 1999. Akt promotes cell survival by phosphorylating and inhibiting a Forkhead transcription factor. Cell **96:**857–868.
2. **Bulavin, D. V., S. Saito, M. C. Hollander, K. Sakaguchi, C. W. Anderson, E. Appella, and A. J. Fornace.** 1999. Phosphorylation of human p53 by p38 kinase coordinates N-terminal phosphorylation and apoptosis in response to UV radiation. EMBO J. **18:**6845–6854.
3. **Degabriele, N. M., U. Griesenbach, K. Sato, M. J. Post, J. Williams, P. K. Jeffery, D. M. Geddes, and E. W. Alton.** 2004. Critical appraisal of the mouse model of myocardial infarction. Exp. Physiol. **89:**497–505.
4. **Donovan, N., E. B. Becker, Y. Konishi, and A. Bonni.** 2002. JNK phosphorylation and activation of BAD couples the stress-activated signaling pathway to the cell death machinery. J. Biol. Chem. **277:**693–696.
5. **Fu, H., R. R. Subramanian, and S. C. Masters.** 2000. 14-3-3 proteins: structure, function, and regulation. Annu. Rev. Pharmacol. Toxicol. **40:**617–647.
6. **Goldman, E. H., L. Chen, and H. Fu.** 2004. Activation of apoptosis signal-regulating kinase 1 by reactive oxygen species through dephosphorylation at serine 967 and 14-3-3 dissociation. J. Biol. Chem. **279:**10442–10449.
7. **Lau, J. M., C. Wu, and A. J. Muslin.** 2006. Differential role of 14-3-3 family members in Xenopus development. Dev. Dyn. **235:**1761–1776.
8. **Liao, P., D. Georgakopoulos, A. Kovacs, M. Zheng, D. Lerner, H. Pu, J. Saffitz, K. Chien, R.-P. Xiao, D. A. Kass, and Y. Wang.** 2001. The in vivo role of p38 MAP kinases in cardiac remodeling and restrictive cardiomyopathy. Proc. Natl. Acad. Sci. USA **98:**12283–12288.
9. **Liu, S., J. F. Wiggins, T. Sreenath, A. B. Kulkarni, J. M. Ward, and S. H. Leppla.** 2006. Dph3, a small protein required for diphthamide biosynthesis, is essential in mouse development. Mol. Cell. Biol. **26:**3835–3841.
10. **Ma, X. L., S. Kumar, F. Gao, C. S. Loudon, B. L. Lopez, A. Christopher, C. Wang, J. C. Lee, G. Z. Feuerstein, and T.-L. Yue.** 1999. Inhibition of p38 mitogen-activated protein kinase decreases cardiomyocyte apoptosis and improves cardiac function after myocardial ischemia and reperfusion. Circulation **99:**1685–1691.
11. **Masters, S. C., and H. Fu.** 2001. 14-3-3 proteins mediate an essential anti-apoptotic signal. J. Biol. Chem. **276:**45193–45200.
12. **Muslin, A. J., and J. M. Lau.** 2005. Differential functions of 14-3-3 isoforms in vertebrate development. Curr. Top. Dev. Biol. **65:**211–228.
13. **Muslin, A. J., and H. Xing.** 2000. 14-3-3 proteins: regulation of subcellular localization by molecular interference. Cell Signal. **12:**703–709.
14. **Muslin, A. J., J. W. Tanner, P. M. Allen, and A. S. Shaw.** 1996. Interaction of 14-3-3 with signaling proteins is mediated by the recognition of phosphoserine. Cell **84:**889–897.
15. **Nishida, K., O. Yamaguchi, S. Hirotani, S. Hikoso, Y. Higuchi, T. Watanabe, T. Takeda, S. Osuka, T. Morita, and G. Kondoh.** 2004. p38α mitogen-activated protein kinase plays a critical role in cardiomyocyte survival but not in cardiac hypertrophic growth in response to pressure overload. Mol. Cell. Biol. **24:**10611–10620.
16. **Otsu, K., N. Yamashita, K. Nishida, S. Hirotani, O. Yamaguchi, T. Watanabe, S. Hikoso, Y. Higuchi, Y. Matsumura, M. Maruyama, T. Sudo, H. Osada, and M. Hori.** 2003. Disruption of a single copy of the p38α MAP kinase gene leads to cardioprotection against ischemia-reperfusion. Biochem. Biophys. Res. Commun. **302:**56–60.
17. **Ren, J., S. Zhang, A. Kovacs, Y. Wang, and A. J. Muslin.** 2005. Role of p38α MAPK in cardiac apoptosis and remodeling after myocardial infarction. J. Mol. Cell Cardiol. **38:**617–623.
18. **Sambrano, G. R., I. Fraser, H. Han, Y. Ni, T. O'Connell, Z. Yan, and J. T. Stull.** 2002. Navigating the signalling network in mouse cardiac myocytes. Nature **420:**712–714.
19. **See, F., W. Thomas, K. Way, A. Tzandis, A. Kompa, D. Lewis, S. Itescu, and H. Krum.** 2004. p38 mitogen-activated protein kinase inhibition promotes cardiac function and attenuates left ventricular remodeling following myocardial infarction in rat. J. Am. Coll. Cardiol. **44:**1679–1689.
20. **Sunayama, J., F. Tsuruta, N. Masuyama, and Y. Gotoh.** 2005. JNK antagonizes Akt-mediated survival signals by phosphorylating 14-3-3. J. Cell Biol. **170:**295–304.
21. **Valks, D. M., S. A. Cook, F. H. Pham, P. R. Morrison, A. Clerk, and P. H. Sugden.** 2002. Phenylephrine promotes phosphorylation of Bad in cardiac myocytes through the extracellular signal-regulated kinases 1/2 and protein kinase A. J. Mol. Cell Cardiol. **34:**749–763.
22. **Xing, H., S. Zhang, C. Weinheimer, A. Kovacs, and A. J. Muslin.** 2000. 14-3-3 proteins block apoptosis and differentially regulate MAPK cascades. EMBO J. **19:**349–358.
23. **Yaffe, M. B., K. Rittinger, S. Volinia, P. R. Caron, A. Aitken, H. Leffers, S. J. Gamblin, S. J. Smerdon, and L. C. Cantley.** 1997. The structural basis for 14-3-3:phosphopeptide binding specificity. Cell **91:**961–971.
24. **Zha, J., H. Harada, E. Yang, J. Jockel, and S. J. Korsmeyer.** 1996. Serine phosphorylation of death agonist BAD in response to survival factor results in binding to 14-3-3 not BCL-X(L). Cell **87:**617–628.
25. **Zhang, L., J. Chen, and H. Fu.** 1999. Suppression of apoptosis signal-regulating kinase 1-induced cell death by 14-3-3 proteins. Proc. Natl. Acad. Sci. USA **96:**8511–8515.
26. **Zhang, S., J. Ren, C. E. Zhang, I. Treskov, Y. Wang, and A. J. Muslin.** 2003. Role of 14-3-3-mediated p38 mitogen-activated protein kinase inhibition in cardiac myocyte survival. Circ. Res. **93:**1026–1028.